Int. J. Electrochem. Sci., 4 **(2009)** 1607 - 1627

International Journal of ELECTROCHEMICAL SCIENCE
www.electrochemsci.org

Using Room Temperature Ionic Liquids as Solvents to Probe Structural Effects in Electro-Reduction Processes. Electrochemical Behavior of Mutagenic Disperse Nitroazo Dyes in Room Temperature Ionic Liquids

Maria Valnice Boldrin Zanoni[1,*], *Emma I. Rogers*[2], *Christopher Hardacre*[3] *and Richard G. Compton*[2]

[1] Department of Analytical Chemistry, Institute of Chemistry, University of São Paulo State, Araraquara, , R. Prof. Francisco Degni, CP 355, 14801-970, SP, Brazil
[2] Department of Chemistry, Physical and Theoretical Laboratory, Oxford University, South Parks Road, Oxford, OX1 3QZ, UK
[3] School of Chemistry and Chemical Engineering/QUILL, Queen's University Belfast, Belfast, Northern Ireland BT9 5AG, UK
[*]E-mail: boldrinv@iq.unesp.br

Received: 16 November 2009 / *Accepted:* 1 December 2009 / *Published:* 31 December 2009

The electrochemical reduction of the disperse azo dyes Red1, Red13 and Orange1 (Or1) was investigated in the RTILs [C_4mim][NTf_2] and [C_4mpyrr][NTf_2], and in contrast with their behavior in conventional aprotic solvents, was shown to proceed via a reversible one electron step to form stable radical anion, which is further reduced at more negative potentials to the dianion. In [C_4mpyrr][NTf_2], cleavage of the N-H bond on the secondary amine was inferred for Orange1, and the ease at which this cleavage occurred is rationalized in terms of acidity of the amine moiety. The ease of reduction was observed to decrease in the order Or1 > Red13 > Red1, and is related to the electron delocalization within the molecule and the electron withdrawing power of the substituents.
The dyes were then oxidized, and Red1 and Red13, bearing an aliphatic amine, were oxidized in a reversible one electron step, to generate the radical cations. The presence of a primary aromatic amine in Or1 provokes a positive shift in the potential of the oxidation peak and shows reversible voltammetry only at scan rates above 200 mV s^{-1}. The ease of oxidation decreases in the order Red1 > Red13 > Or1, and is thought to relate to the detected mutagenic activity of the dyes.

Keywords: diperse dyes, room temperature ionic liquid, electrochemical reduction, electrochemical oxidation, mutagenic dyes

1. INTRODUCTION

Although, the majority of commercial textile dyes are water-soluble (hydrophilic), disperse dyes are a category of hydrophobic dyes and are heavily employed for dyeing polyester fabrics[1]. Previous studies [2-20] have suggested that some nitro azo dyes from this family of dye, as well some intermediates or generated products during metabolization can be catalogued as a novel class of mutagenic compounds. Particularly, some derivatives of disperse azo dyes have been isolated and identified as mutagenic contaminants in Japanese rivers [3-5, 9, 10, 18-20], Brazilian textile effluents, river water, sediment and in drinking water[2, 6-8, 11, 13-17]. These species are easily transported in aqueous systems and have a tendency to bio-accumulate in sediments, soils and may subsequently end up in drinking water treatment plants.

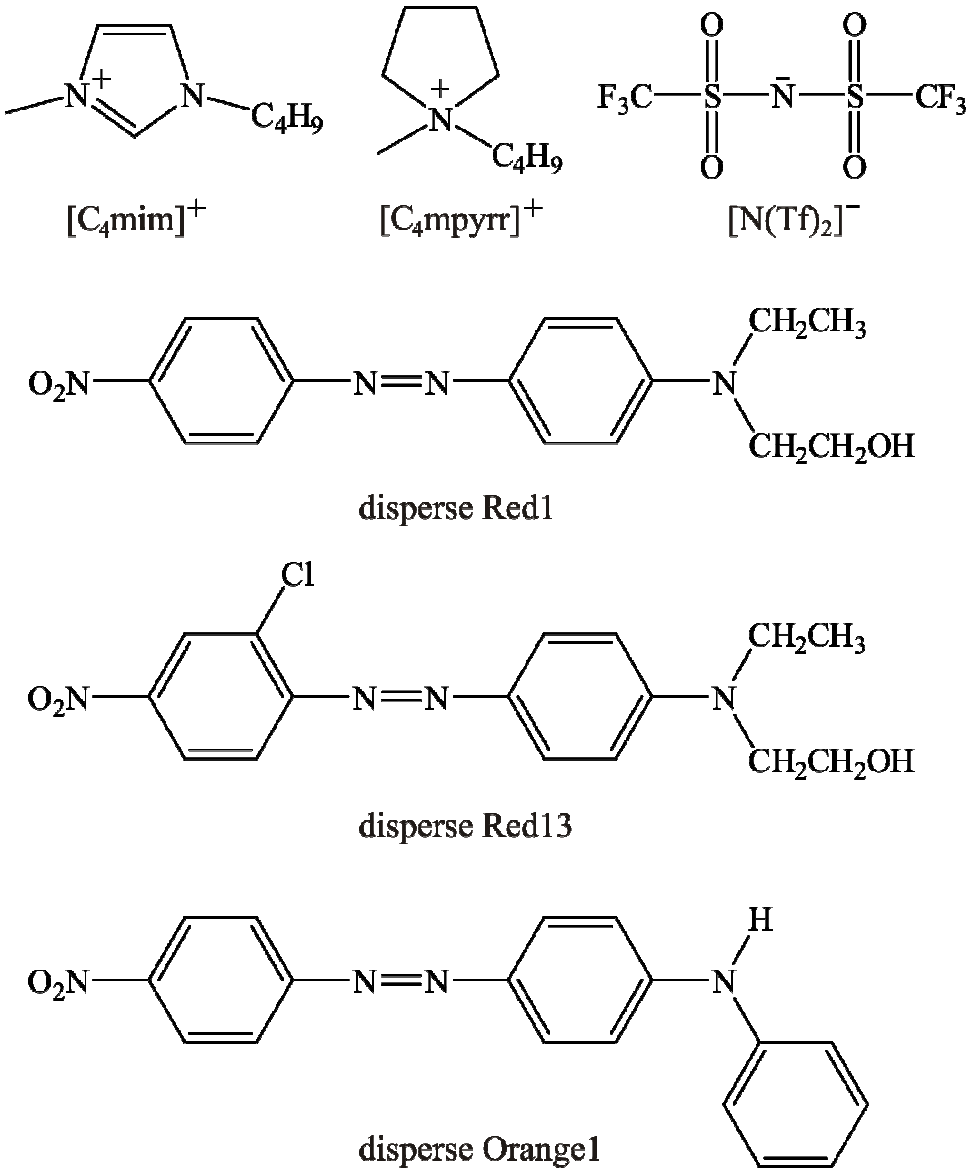

Figure 1. Chemical structures of the cations and anion used as the RTIL and the dyes used in this study.

It is well known that the toxicity and carcinogenicity of certain azo dyes in mammalian systems may result either from interactions of the intact molecules with cytosolic receptors or from the formation of free radicals and arylamines during azoreduction[21-24]. Azoreduction in mammalian systems is catalysed by hepatic enzymes in the liver and by bacteria in the intestinal tract. Reduction of azo dyes may produce compounds with decreased or increased toxic or carcinogenic effects, compared to the parent molecule. Therefore, elucidation of electrochemical mechanisms of the reduction and oxidation at an electrode surface can be used to suggest mechanisms for the biochemical behaviour of disperse dyes, *i.e.* the electrode reactions can serve as models for the biological pathway, or they can be used to generate intermediates able to induce DNA damage, allowing study of the biological implications of the redox-activation step.

The special characteristics of room temperature ionic liquids (RTILs) for electrochemical applications have been the focus of several researchers[25-28]. They are robust, present good conductivity, exhibit wide electrochemical potential windows[29, 30] and, as materials composed of cations and anions, are able to solvate a large variety of organic and inorganic compounds, either polar or non-polar. In addition, some authors have evidenced strong stabilization of electrogenerated radical anions by the cation of the RTIL[31-35], which affects the kinetics of electron transfer itself and minimises associated chemical reactions. Therefore, RTILs can constitute an excellent solvent to investigate structural effects operating in the electrochemical behaviour of disperse dyes.

The aim of the present work was to study the electrochemical behaviour of three disperse dyes: disperse Red1 (C.I. 11110), disperse Orange1 (C.I. 11080) and disperse Red 13 (C.I. 11115) dyes, with the chemical structures shown in Figure 1. The dyes were chosen as model compounds for disperse azo dyes bearing the nitro and amino ring substituent groups. The electrochemical reduction and oxidation of the selected dyes were investigated in the room temperature ionic liquids 1-butyl-3-methylimidazoloium bis(trifluoromethanesulfonyl)imide, $[C_4mim][NTf_2]$ and *N*-butyl-*N*-methyl-pyrrolidinium bis(trifluoromethanesulfonyl)imide $[C_4mpyrr][N(Tf)_2]$ (Fig.1) using Pt microelectrodes. A quantitative interpretation of the mechanism in $[C_4mim][NTf_2]$ was carried out using digital simulation techniques (DigiSim® 3.03, BAS Technicol), and appropriate best-fit parameters determined and reported below.

2. EXPERIMENTAL PART

2.1. Chemical reagents

$[C_4mim][N(Tf)_2]$, 1-butyl-3-methylimidazolium bis(trifluoromethanesulfonyl)imide and $[C_4mpyrr][N(Tf)_2]$, *N*-butyl-*N*-methylpyrrolidinium bis(trifluoromethanesulfonyl)imide were prepared by standard literature procedures[36]. Disperse Red1 (C.I. 11110), disperse Orange1 (C.I. 11080) and disperse Red13 (C.I. 11115) dyes was purchased from Aldrich (99.5%) and dissolved directly in the ionic liquid, submitted to sonication for thirty minutes and used freshly. Guanine solution was made by dissolving the respective salt, (Aldrich, 99.5%), in the ionic liquid using the same procedure.

2.2. Instrumental

Electrochemical experiments were performed using a computer controlled μ-Autolab potentiostat (Eco-Chimie, Netherlands). A conventional two-electrode arrangement was employed, with a platinum working electrode (10 μm diameter) and a silver wire (0.5 mm diameter, Goodfellow Cambridge Ltd.) quasi reference electrode. The Pt electrode was polished with diamond pastes (Kemet, UK) of decreasing particle size (3 - 0.1μm) on soft lapping pads, followed by polishing with 1 μm and 0.01 μm alumina slurries on lapping pads. The electrode diameter was calibrated electrochemically by recording voltammograms of a 2 mM solution of ferrocene (Fc) in acetonitrile containing 0.1 M TBAP, using a scan rate of 10 mV s^{-1} and diffusion coefficient value of 2.3 x 10^{-9} m^2s^{-1} at 293 K[37] for ferrocene.

A small section of disposable micropipette tip was used to modify the clean microdisk, creating a cavity into which 20 μL of ionic liquid solvent was placed. The electrodes were housed in a glass T-cell [38] specially designed for investigating microsamples of ionic liquids under controlled atmospheres. The RTIL solutions were de-gassed under vacuum (Edwards High Vacuum Pump, Model ES 50) for *ca.* 120 min, to remove trace atmospheric moisture and dissolved gases naturally present in the ionic liquid. All experiments were conducted in a Faraday cage, thermostated at 298 K, where background noise was minimized.

For experiments involving ferrocene as an internal reference probe, 7 μL of a solution of 10 mM of Fc in acetonitrile was pipette into 20 μL of guanine/RTIL solution inside the T-cell. The acetonitrile was evaporated during the 120 minute vacuum purgation (Edwards High Vacuum Pump, Model ES 50) to give an overall Fc concentration of 3.5 mM.

Chronoamperometric experiments were achieved using a sample time of 0.1 s. The potential was held at point corresponding to zero current for 20 s pre-treatment, after which the experimental transients were obtained by stepping to a potential just after the peak and measuring the current for 10 s. Fitting of the experimental data was achieved using the non-linear curve fitting function (Origin 7.0, Microcal Software Inc.), following the Shoup and Szabo[39] approximation, as employed previously[40-42]. The software was instructed to perform 100 iterations on the data, fixing the value for the electrode radius calculated by voltammetric calibration of ferrocene.

3. RESULTS AND DISCUSSION

3.1. Electrochemical reduction of disperse Red1, disperse Red13 and disperse Orange 1 in [C_4mim][NTf_2]

The electrochemical reduction of 0.88 mM disperse Red1 (Red1), disperse Red13 (Red13) and disperse Orange1 (Or1) in dimethylformamide (DMF) plus 0.1 mol L^{-1} tetra-*n*-butylammonium tetrafluoborate (Bu_4NBF_4) at a Pt electrode is shown in Figure 2, as an example of voltammetry in an aprotic medium. The reduction of the nitro group to its radical anion is observed on first cathodic wave (I_c) for all investigated dyes (-0.69 V *vs* Ag/AgCl for Red13; -0.79 V for Orange1 *vs* Ag/AgCl and -0.84 V *vs* Ag/AgCl for Red1), with a corresponding anodic peak (I_a) at all scan rates investigated (10 -

500 mVs^{-1}). The magnitude of the subsequent reduction step (II_c) to form the dianion decreases markedly from Orange1 (-0.97V) to Red1 (-1.06 V) and is almost absent in Red13 dye reduction, hinting at subsequent chemical reactions suppressing further reduction at more negative potentials. A shoulder at less negative potential is observed on voltammograms recorded for Orange1 (-0.68V) and Red1 (-0.68V) and is possibly due to adsorption of the reductive product[43]. In order to get more information about the reductive mechanism and to improve stabilization of anion radical and dianion for further biological investigations the electrochemical reduction in RTILs was investigated with the expectation that reaction with the solvent/supporting electrolyte might be reduced.

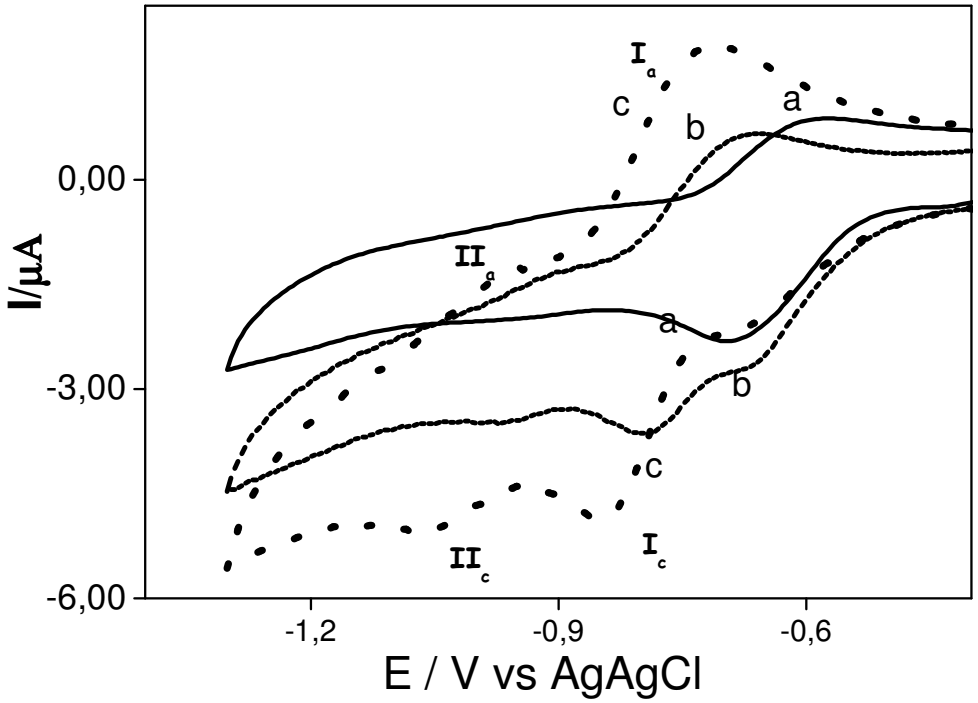

Figure 2. Cyclic voltammograms for 0.88 mM (a) disperse Red13, (b) disperse Orange1 and (c) disperse Red1 in DMF plus 0.1 mol L^{-1} Bu_4NBF_4 on a Pt electrode at a scan rate of 50 mV s^{-1}.

Figure 3 shows cyclic voltammograms obtained for the reduction of 10 mM Red13 (Curve X); Red1 (Curve Y) and Or1 (Curve Z) dyes on a Pt microelectrode in [C_4mim][NTf_2] at 100 mV s^{-1}. The voltammetric behavior for each dye is very similar and shows two well-defined reduction peaks (I_c and II_c), likely due to the reduction of nitro group to form the radical anion ($NO_2^{\bullet -}$) and dianion (NO_2^{2-}), and two corresponding anodic peaks (I_a and II_a) on the reverse potential scan at all scan rates (10 - 1000 mV s^{-1}).

Steady-state behavior is obtained only at scan rates below 20 mVs^{-1} (Curve 1 Figure 4, which is representative of Red13 behavior) and becomes more transient-shaped at scan rates above 50 mVs^{-1}. Under the latter conditions, the ratio of anodic-to-cathodic peak heights for each redox couple (I_a/I_c and II_a/II_c) are close to 1 at all scan rates studied and are independent of substrate concentration and

potential scan rate; classic behavior for two reversible one electron reduction processes. For the faster scan rates, a linear relationship is obtained for plots of peak currents (I_c and II_c) *vs* square-root of the scan rate, indicating that both processes are diffusion-controlled. The reversibility observed for both reductive peaks contrasts with the behavior described for the reduction of nitrobenzene in [C_4dmim][NTf_2] [26, 44, 45] and other aprotic solvents[46, 47], where there is formation of a stable radical anion (peak 1), followed by an irreversible chemical process (peak 2) involving the formation of the dianion, rapid protonation and nitrosobenzene generation. The high stability of the radical anion is likely due to the high delocalization of the negative charge from the nitro group. The presence of the acidic proton on the C(2) position of the $[C_4mim]^+$ (1-butyl-3-methylimidazolium) cation, and the basic nature of the dianion produced during the second reduction step suggests that the solvent cation might act as a proton donor, but here it is seen a neglected influence.

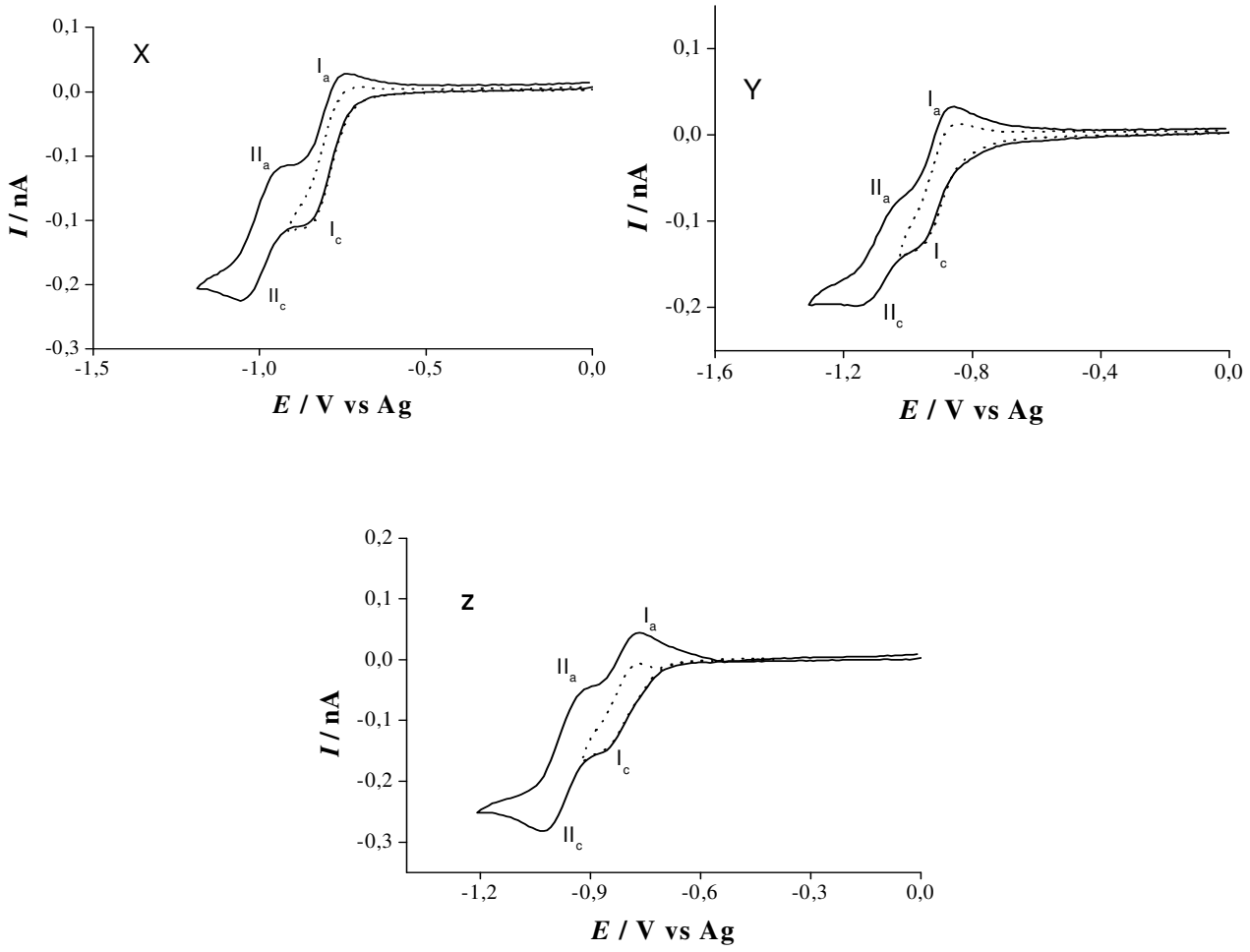

Figure 3. Cyclic voltammograms for the reduction of 10 mM Red13 (X), Red1 (Y) and Orange1 (Z) in [C_4mim]NTf_2] on Pt microelectrode at a scan rate of 100 mV s^{-1}.

Chronoamperometric transients were recorded for the reduction of 10 mM Red13, Red1 and Or1 dyes in [C_4mim][NTf_2] in which the potential was stepped from 0 V to -0.9 V *vs* Ag and 0 V to -1.1 V for Red13, 0 V to –1.0 and 0 V to -1.25 V for Orange1 and 0 to –0.95 V and 0V to -1.3 V for Red1. The experimental curves were analysed in terms of the Shoup and Szabo equation, as described previously[39, 41, 42], and an example of the experimental (–) and theoretical (○) transients observed are shown in the inset of Figure 4 for the first (I) and second (II) reduction of Red13. Excellent fitting was observed for all transients, and the number of electrons transferred was calculated as close to one (0.88 ± 0.044 for Red1, 1.02 ± 0.173 for Red13 and 0.89 ± 0.102 for Or1) for the first wave and close to two electrons (2.12 ± 0.89 for Red1, 1.95 ± 0.060 Red13 and 1.87 ± 0.33 for Or1) for the first and second wave together. The diffusion coefficients obtained from chronoamperometry were (2.13 ± 0.15) x 10^{-8} cm^2 s^{-1} for Red1, (2.63 ± 0.10) x 10^{-8} cm^2 s^{-1} for Red13 and (2.93± 0.44) x 10^{-8} cm^2 s^{-1} for Or1. The values are very similar, but smaller than those observed in conventional organic solvents, likely due to the difference in the viscosity of the solvents, leading to much slower diffusion in the more viscous ionic liquids.

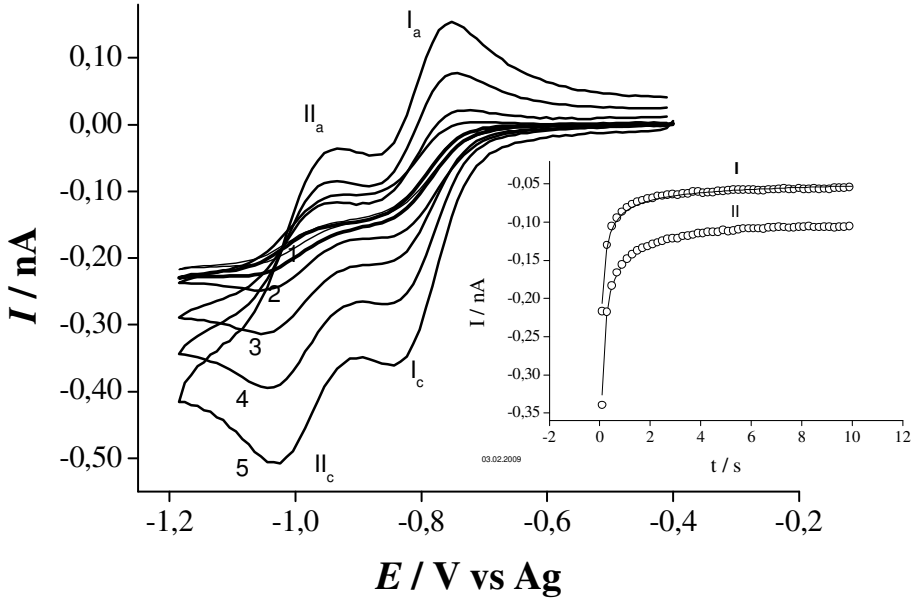

Figure 4. Cyclic voltammetry for 10 mM Red13 in [C_4mim][NTf_2] at scan rates of (1) 10, (2) 20, (3) 50, (4) 100 and (5) 200 mV s^{-1}. Inset: Chronoamperometric transients for the reduction of Red13 in [C_4mim][NTf_2] from I) 0 to -0.90V and II) 0 to -1.1V.

The use of a Ag wire quasi-reference has been shown to cause shifts in potential over the experimental timescale, and so, in order to obtain reliable potential values for simulation purposes (see Section 3.2), the reduction of 10 mM Red1, Red13 and Or1 dyes in [C_4mim][NTf_2] was studied by cyclic voltammetry using ferrocene/ferrocenium (Fc/Fc^+) couple as internal reference, widely used as a well-defined redox system in most ionic liquids[48]. Orange1 appears to be the most easily reduced

(at a potential E_I of -0.44 ± 0.01 V *vs* Fc/Fc^+) followed by Red13 (-0.46 ± 0.02 V *vs* Fc/Fc^+) and finally Red1 (-0.52 ± 0.02 V *vs* Fc/Fc^+), with peak potentials for the second reduction wave, E_{II} of -0.67 ± 0.02 V *vs* Fc/Fc^+ for Or1, -0.66 ± 0.01 V *vs* Fc/Fc^+ for Red13, and -0.74 ± 0.02 V *vs* Fc/Fc^+ for Red1. The peak separation between peak I and II in each case are 229 mV (Or1), 198 mV (Red13) and 226 mV (Red1). This may represent the different electron withdrawing power of the substituents in the dye analysed. The lower potential required for the reduction of disperse Red13 compared to disperse Red1 suggests that the –Cl substitutent in the *ortho* position in Red13 is important, and has a deactivating effect on the electrophilic activity of the nitro group in the molecule, since both dyes have the same nitro group (electron withdrawing effect) and tertiary amine (–N $(CH_2CH_3)(CH_2CH_2OH)$) (electron donating effect) as substituents. On the other hand, the electrophilicity on the nitro group is dramatically reduced in disperse Orange1 because of the aromatic amine substituent (electron withdrawing and mesomeric effects), leading to a decrease in the charge on the nitro group.

It is shown in the literature[23, 24] that a knowledge of the electrochemical reduction of substituted azobenzenes by cyclic voltammetry can be a useful model for microsomal azoreductase mechanism. The mutagenic responses of the three disperse dyes for the strain TA 98 in the assays without exogenous metabolization, indicates that the disperse Red1 is the most mutagenic (with potency of 4 revert/µg), followed by disperse Red13 (0.4 revert/µg) and disperse Orange1 (0.2 revert/µg) [49]. These results are in contrast with the reductive facility of the nitro group observed in the molecule. It is important to understand the electrophilic character of the molecule or its derivative since the main characteristic of environmental genotoxic mutagens can increase the possibility of reaction with nucleophilic sites of the DNA, leading to adduct formation[50]. The use of RTILs as solvents allows us to study the electrochemical parameters of the dye and the effect of chemical structure of such parameters, with less interference of rapid chemical complications.

In order to check the reductive mechanism and to estimate the standard electrochemical constants involved in the electrochemical reduction of disperse Red1, disperse Red13 and disperse Or1 dyes in $[C_4mim][NTf_2]$, digital simulation methods were utilized and best fit parameters deduced, as described in Section 3.2.

3.2. Modelling the reduction of disperse Red1, disperse Red13 and disperse Orange 1 in $[C_4mim][NTf_2]$ in DigiSim®

The one-dimensional diffusion simulation program available in DigiSim® (BAS Technicol) [51] was used to successfully model the cyclic voltammograms for the reduction of 7 mM disperse Red1, disperse Red13 and disperse Orange1 in $[C_4mim][NTf_2]$. Scan rates ranging from 10 mV s^{-1} to 2000 mV s^{-1} were studied experimentally and simulated using the hemispherical diffusion model [52], following the mechanism below (Scheme 1), involving the reduction of the neutral species to the radical anion (1) followed by the reduction of this species to the dianion (2):

$$E_1: [O_2NC_6H_4N{=}NC_6H_4NR_1R_2] + e^- \rightarrow [O_2NC_6H_4N{=}NC_6H_4N\ R_1R_2]^{\bullet -} \quad (1)$$

$$E_2: [O_2NC_6H_4N{=}NC_6H_4N\ R_1R_2]^{\bullet -} + e^- \rightarrow [O_2NC_6H_4N{=}NC_6H_4N\ R_1R_2]^{2-} \quad (2)$$

where R_1 = (CH_2CH_3) and R_2 = ($CH_2CH_2CH_3$) in Red1 and Red13 and R_1 = (H) and R_2 = (C_6H_5) in Or1 dye. The experimental (–) and theoretical (○) voltammograms at scan rates of 10 mV s^{-1}, 100 mV s^{-1} and 1000 mV s^{-1} are shown in Figure 5 for Orange1, Figure 6 for Red13 and Figure 7 for Red1. The above mechanistic scheme allowed good fits to be achieved for waves I and II of both the forward and reverse scans, even without accounting for ion-pairing effects. This result indicates that all the disperse nitro dyes studied are reduced initially to their corresponding anion radicals during the first cathodic step (Equation 1). The second cathodic step arises when these anion radicals are reduced to the stable dianion.

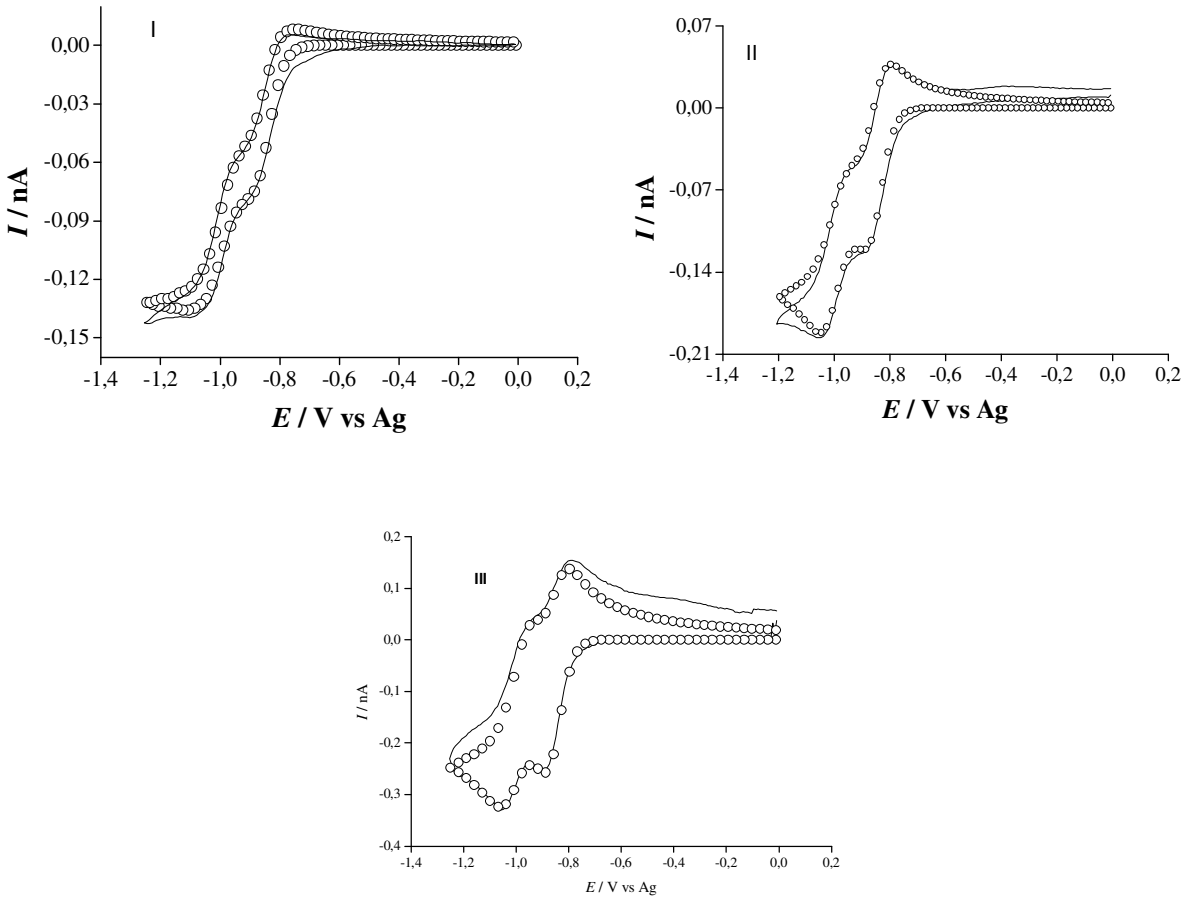

Figure 5. Comparison of the experimental (–) and simulated (○) cyclic voltammograms for the reduction of 10 mM of Or 1 in [C_4mim][NTf_2] at scan rates of (I) 10 mV s^{-1}; (II) 100 mV s^{-1} and (III) 1000 mV s^{-1} on a Pt microeleectrode (radius 6.03μm).

The optimized parameters for the best fits to the experimental data (Figures 5-7) were calculated and the average values of the three scan rates investigated are compiled in Table 1. Values

of charge-transfer coefficient (α) and electrode radius (r_d) were fixed as 0.50 and 6.03 μm, respectively. From the data it is observed that the electrochemical rate constant, k^0_1, obtained by simulation are approximately the same order of magnitude but slightly smaller for Red1 dye. The ratio of diffusion coefficients, γ, where $\gamma = D_B/D_A$, D_A is the diffusion coefficient of the neutral species and D_B is the diffusion coefficient of the radical anion species, is calculated as close to 0.1. These values are a lot lower than those expected in conventional solvents, where values closer to unity are observed. The high ratios arise due to the ionic nature of the solvent, in which the charged species (radical anion) diffuses much more slowly that the neutral species (parent molecule), due to the increased strength of the Coulombic forces between the RTIL cation and the radical anion, compared to that with the neutral molecule. This phenomenon is negligible in more conventional aprotic solvents, but has been observed previously for other compounds in various RTILs [26, 34, 35].

Next, the oxidation of the three dyes was carried out in $[C_4mim][NTf_2]$, focusing on the oxidation of amino group in Red1, Red13 and Or1 dyes.

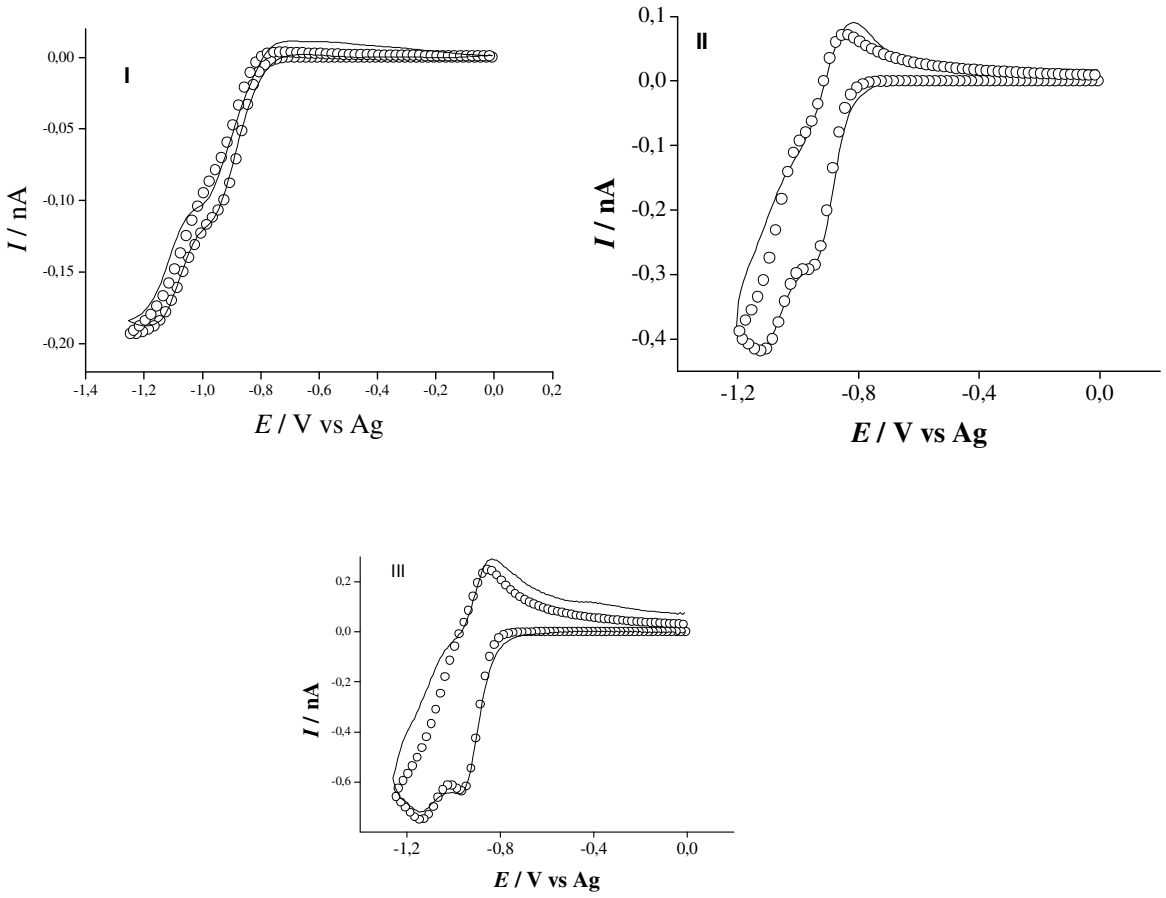

Figure 6. Comparison of the experimental (–) and simulated (○) cyclic voltammograms for the reduction of 10 mM Red13 in $[C_4mim][NTf_2]$ at scan rates of (I) 10 mV s^{-1}; (II) 100 mV s^{-1} and (III) 1000 mV s^{-1} on a Pt microelectrode (radius 6.03μm).

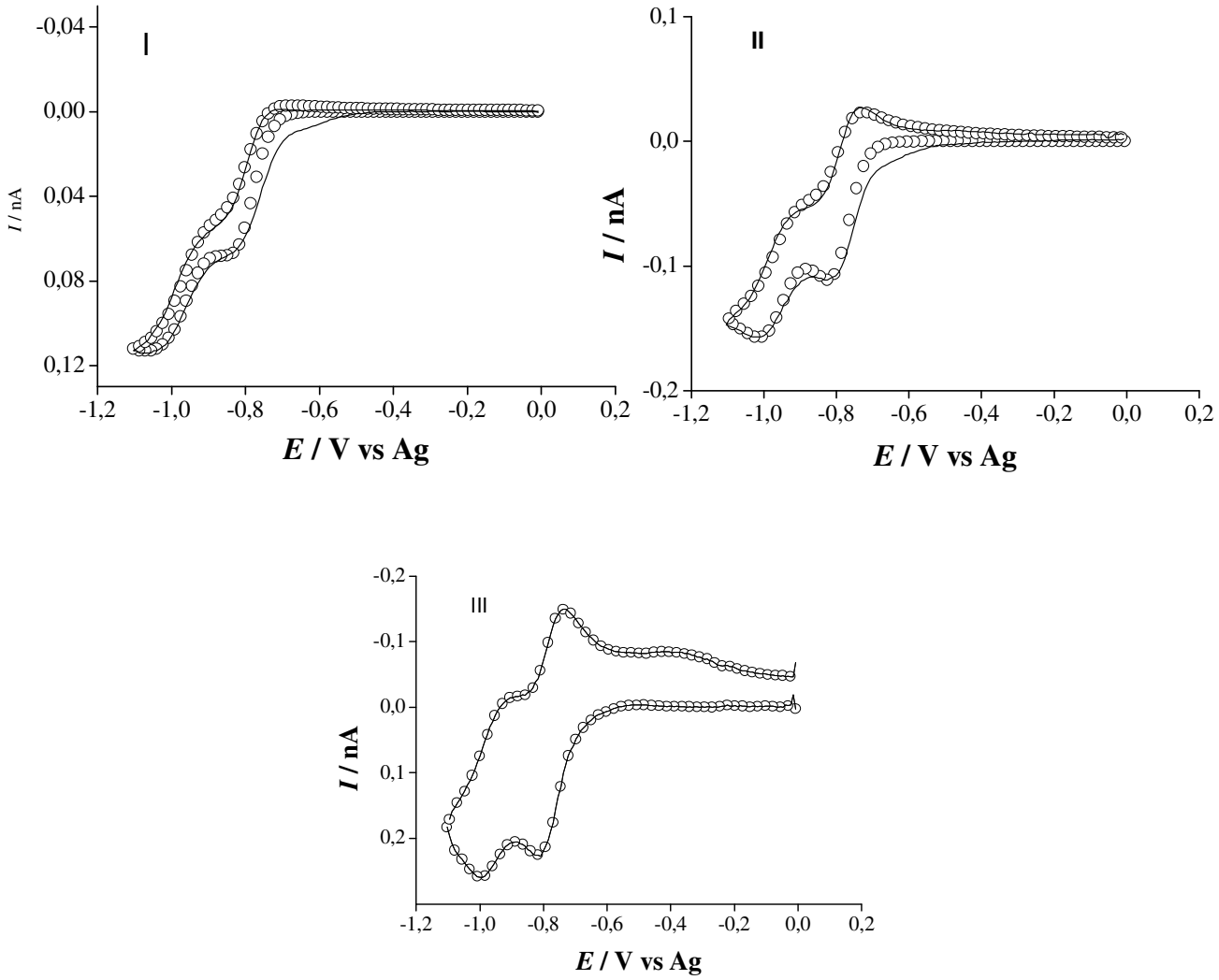

Figure 7. Comparison of the experimental (–) and simulated (○) cyclic voltammograms for the reduction of 10 mM Red1 in $[C_4mim][NTf_2]$ at scan rates of (I) 10 mV s^{-1}; (II) 100 mV s^{-1} and (III) 1000 mV s^{-1} on a Pt microelectrode (radius 6.03μm).

Table 1. Best fit parameters employed in the DigiSim® simulation of reduction voltammetry of disperse nitro dyes in $[C_4mim][NTf_2]$ on a 10μm diameter Pt electrode

DYES	ORANGE 1	RED 13	RED1
[A]/ x10^{-3}mol l^{-1}	8.69 ± 0.04	5.90 ± 0.08	27.4 ± 0.05
D_A/ x10^{-8} cm^2 s^{-1}	2.93 ± 0.03	1.96 ± 0.02	1.83 ± 0.03
D_B/ x10^{-9} cm^2 s^{-1}	3.07 ± 0.01	2.60± 0.04	7.90 ± 0.05
D_c/ x10^{-9} cm^2 s^{-1}	1.22± 0.03	4.85± 0.08	1.20± 0.01
k^0_1/cm s^{-1}	0.00510 ± 0.0003	0.00560 ± 0.0002	0.00167± 0.0004
k^0_2/cm s^{-1}	0.00170± 0.0001	0.00310± 0.0002	0.00068± 0.0001
$E^0_{f,1}$/V	-0.876 ± 0.005	-0.881 ± 0.006	-0.946 ± 0.001
$E^0_{f,2}$/V	-0.986 ± 0.004	-0.993± 0.008	-0.980± 0.007

3.3. Electrochemical oxidation of disperse Red1, disperse Red13 and disperse Orange1 in [C_4mim][NTf_2]

Figure 8 shows the cyclic voltammograms obtained for oxidation of 10 mM Red13 (Curve X), Red1 (Curve Y) and Or1 (Curve Z) on Pt microelectrode in [C_4mim][NTf_2] at 100 mV s^{-1}. Only one defined oxidation peak (I_a) is observed, which is attributed to the oxidation of the amine group present in all investigated dye molecules. Electrochemically reversible voltammetry is observed for the oxidation of Red1 and Red13 dye bearing secondary aliphatic amines. A plot of peak current *vs* square-root scan rate shows a linear relationship as expected for diffusion-controlled processes. The primary aromatic amine present as a *para* substituent in the disperse Orange1 dye leads to a shift in the oxidation wave to more positive potentials than observed for Red1 and Red13. A plot of peak current *vs* square-root scan rate shows a linear relationship only at high scan rate and the voltammogram exhibits a small cathodic peak on the reverse scan only at 200 mVs^{-1}, suggesting that a slow chemical reaction is consuming the generated product.

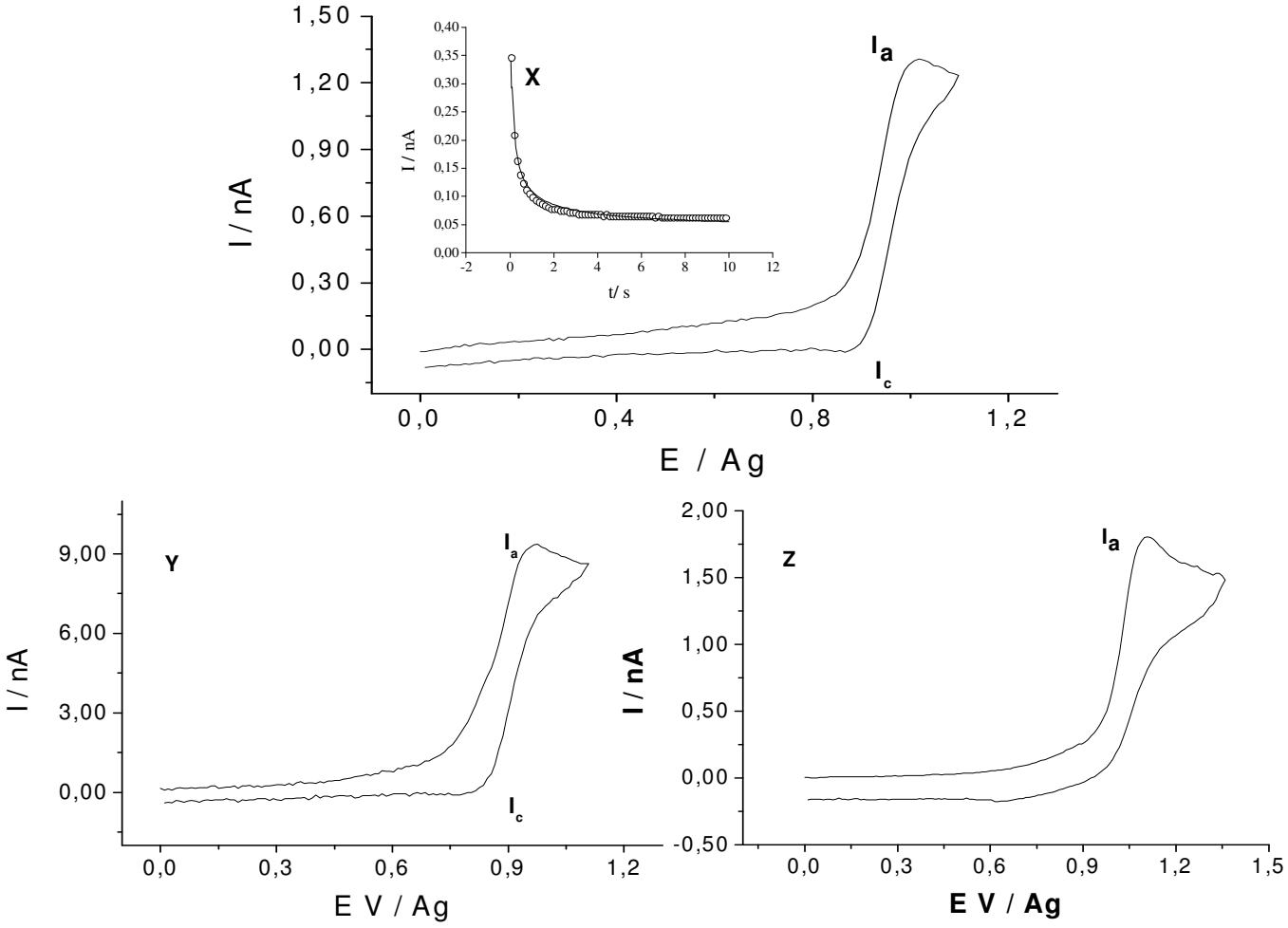

Figure 8. Cyclic voltammograms for the oxidation of 10 mM Red13 (X), Red1 (Y) and Orange1 (Z) in [C_4mim]NTf_2] on a Pt microelectrode at s scan rate of 100 mV s^{-1}. Inset shows the chronoamperometric transient for Red1. The potential was stepped from +0.2 to 1.1 V.

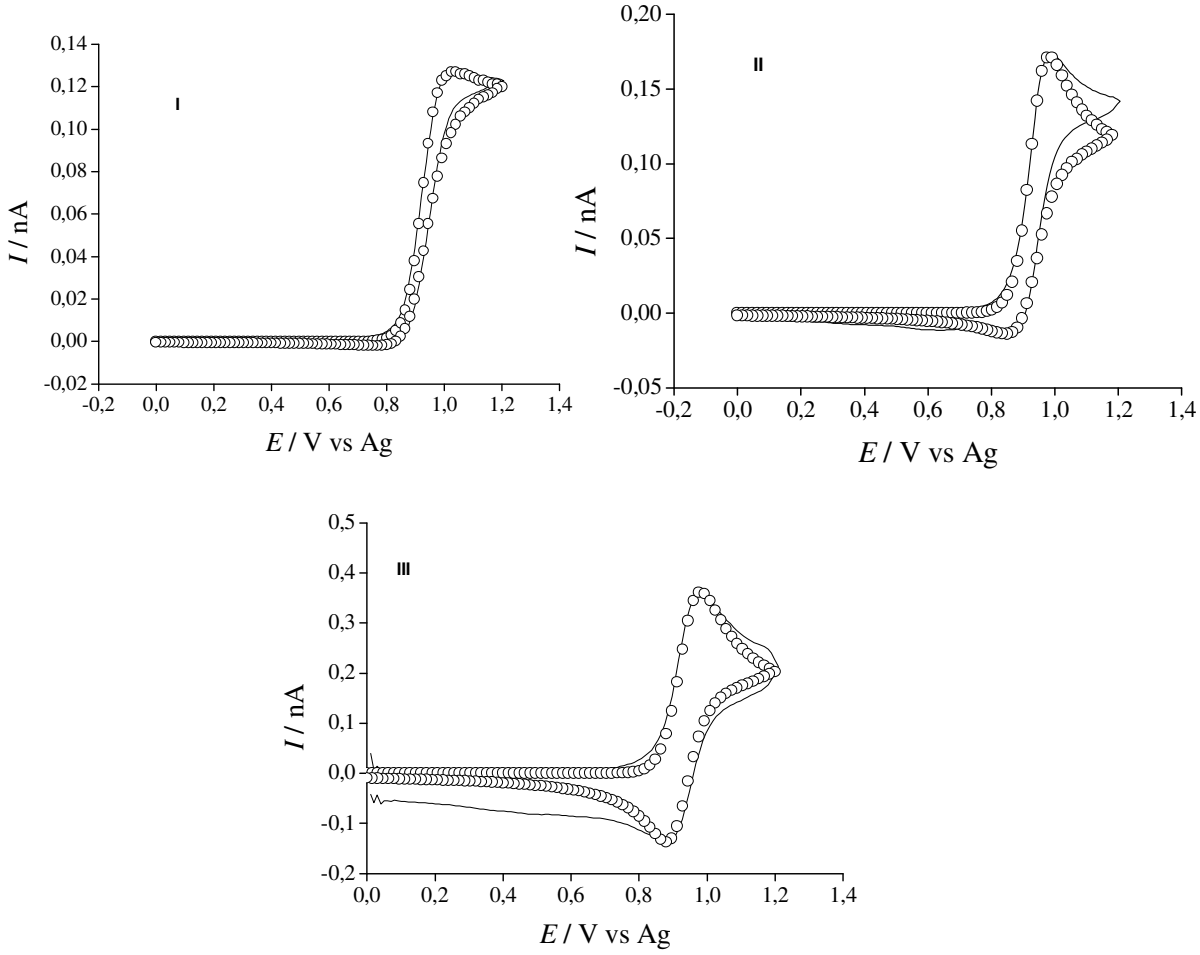

Figure 9. Comparison of the experimental (–) and simulated (○) cyclic voltammograms for the oxidation of 10 mM of Red1 in [C_4mim][NTf_2] at scan rates of (I) 10 mV s^{-1}; (II) 100 mV s^{-1} and (III) 1000 mV s^{-1} on Pt microelectrode (radius 6.03µm).

The cyclic voltammetric behavior was studied versus an internal redox couple of Fc/Fc^+ at scan rates from 10 to 1000 mV s^{-1}. The average of the half-wave potentials of the redox couple was measured in relation to Fc/Fc^+ added to the solution and the values were almost constant (deviation of 1 - 4 mV) over the whole scan rate range for all dyes and were estimated as +0.57 ± 0.003 V *vs* Fc/Fc^+ for Red1, +0.62 ± 0.007 V *vs* Fc/Fc^+ for Red13 and +0.72 ± 0.010 V *vs* Fc/Fc^+ for Or1. The susceptibility for oxidation of each dye is related to the chemical structure. The lower oxidation potential of disperse Red1 and disperse Red13 is a result of the electron-donating substituent present in the structure. Disperse Orange1 bears a phenyl ring on the amine group, *i.e.* an electron-withdrawing substituent, and requires high positive potential to be oxidized. The ease of oxidation decreases in the order Red1 > Red13 > Or1, and this is directly related to the mutagenic activity [53] of the dye and ultimately the presence of electron withdrawing substituents within the amine moiety.

Before attempting to model any cyclic voltammetry, accurate diffusion coefficients and concentrations of each disperse dye in $[C_4mim][NTf_2]$ were obtained by chronoamperometry. The potential was stepped from 0.2 V to a potential of +1.1 V (Red1), +1.3 V (Orange1) and +1.2V (Red13) and the transients fitted to the Shoup and Szabo expression. An example of the experimental (–) and theoretical (○) transients is presented in the inset of Figure 8 (X) for Red13. The diffusion coefficients obtained from chronoamperometry are approximately similar, with values of (7.57 ± 0.25) x 10^{-8} cm^2 s^{-1} for Red 1, (9.26± 0.10) x 10^{-8} cm^2 s^{-1} for Red13 and (9.93± 0.44) X 10^{-8} cm^2 s^{-1} for Or1 and the number of electrons transferred is close to one (1.02 ± 0.14 for Red1, 0.72 ± 0.173 for Red13 and 0.87 ± 0.102 for Or1), suggesting the initial formation of a radical cation. The electrochemical behavior observed indicates that the oxidation of the amino group in Red1 and Red13 dyes generates a stable radical cation, probably stabilized by charge delocalization. Meanwhile the radical cation of Orange1 is not reduced on the reverse scan possibly due to either ion-pair association or dimerization reactions, involving the formation of the free radical due loss of hydrogen from the primary amine.

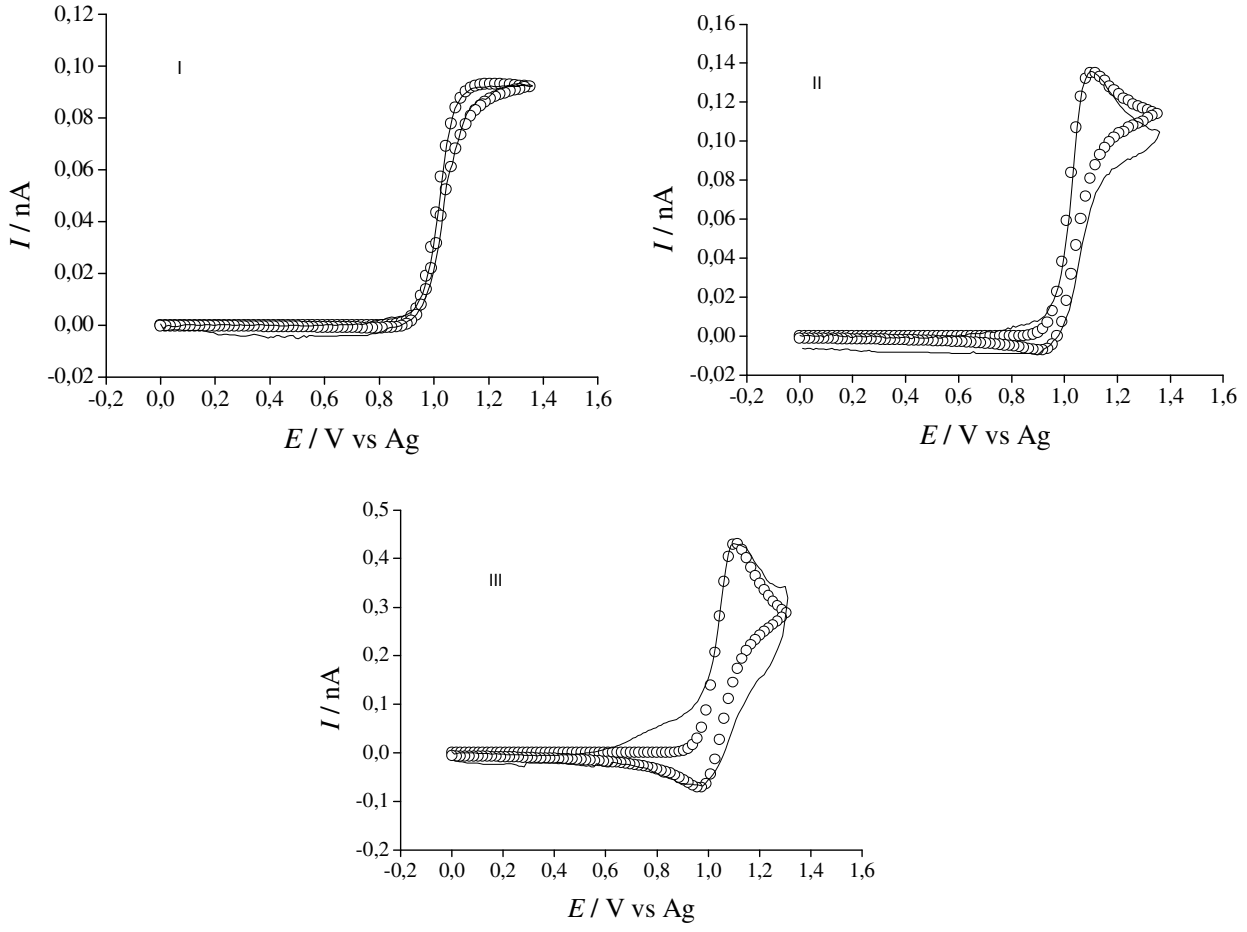

Figure 10. Comparison of the experimental (–) and simulated (○) cyclic voltammograms for the oxidation of 10 mM of Orange 1 in $[C_4mim][NTf_2]$ at scan rates of (I) 10 mV s^{-1}; (II) 100 mV s^{-1} and (III) 1000 mV s^{-1} on Pt microelectrode (radius 6.03µm).

3.4. Modelling the oxidation of disperse Red1, disperse Red13 and disperse Orange1 in [C_4mim][NTf_2]

Next, the voltammetry for the oxidation of Red1, Red13 and Or1 dyes in [C_4mim][NTf_2] ionic liquid was simulated using the DigiSim® program described previously [50,54]. The simulated voltammograms for the oxidation of each dye (at scan rates of 10, 100 and 1000 mV s^{-1}) were obtained using fixed values of α (= 0.5) and electrode radius, r_d (6.03 μm, obtained by calibration with 2 mM of Fc/Fc^+ redox couple in acetonitrile) and adjusting the concentration, c, formal electrode potential, E_f, and diffusion coefficients of A and B, D_A and D_B, where A is the neutral parent molecule and B is the radical cation. Figures 9, 10 and 11 show the best theoretical fits (○) to the experimental data (–) for the oxidation of 10 mM Red1, Red13 and Or1 dyes in [C_4mim][NTf_2] on a Pt microelectrode. Excellent theoretical fitting to the experimental data was observed, supporting a mechanism where the amine group is oxidized with the transfer of one electron. Table 2 shows the best fit electrochemical parameters obtained using the method described above. Diffusion coefficients for species A, D_A are of the same order of magnitude for Red1 Red13 and Or1 dyes with values around 10^{-8} cm^2 s^{-1}. For all dyes the values of $\gamma = D_B/D_A$ are very close to 0.10. In addition, the values of k_0 are approximately the same order of magnitude, suggesting small influences of structure change within the dye molecule.

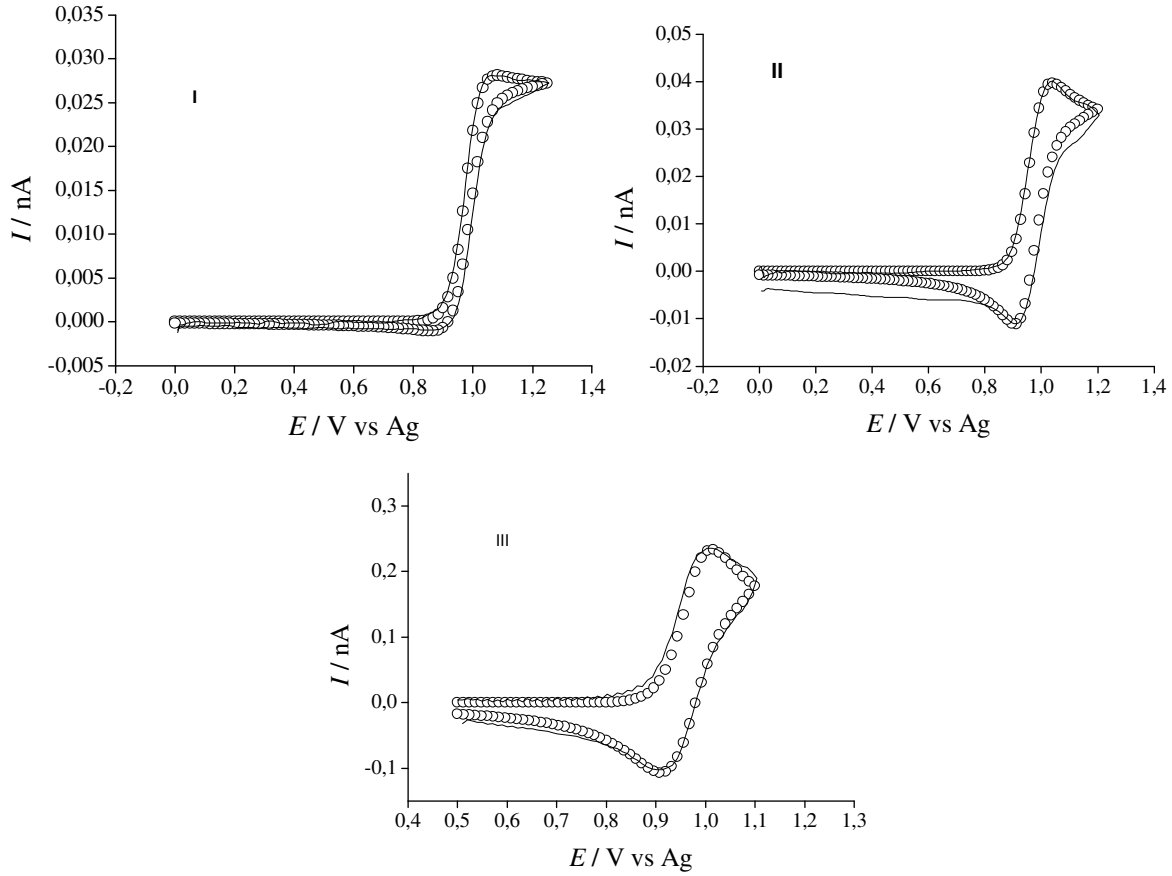

Figure 11. Comparison of the experimental (–) and simulated (○) cyclic voltammograms for the oxidation of 10 mM of Red 13 in [C_4mim][NTf_2] at scan rates of (I) 10 mV s^{-1}; (II) 100 mV s^{-1} and (III) 1000 mV s^{-1} on Pt microelectrode (radius 6.03μm).

Table 2. Best fit parameters employed in the simulation of oxidation voltammetry of disperse nitro dyes in [C_4mim][NTf_2] on a 10μm diameter Pt electrode

DYES	ORANGE 1	RED 13	RED1
[A]/ x10^{-3}mol l^{-1}	34.12 ± 0.14	13.76 ± 0.14	35.17 ± 0.05
D_A/ $_X10^{-8}$ cm^2 s^{-1}	9.70 ± 0.22	9.43 ± 0.05	9.46 ± 0.45
D_B/ $_X10^{-9}$ cm^2 s^{-1}	14.5 ± 1.01	9.35 ± 2.04	10.25 ± 1.05
k^0_1/cm s^{-1}	0.00333 ± 0.005	0.00443 ± 0.006	0.00217± 0.0010
$E^0_{f,1}$/V	-1.075 ± 0.020	-0.985 ± 0.060	-0.965 ± 0.010

3.5. Electrochemical reduction of disperse Red1, disperse Red13 and disperse Orange1 in [C_4mpyr][NTf_2]

Taking into consideration the observation that RTILs can act as hydrogen-bond donors and acceptors, with acidity related to the nature of the cation, further studies were carried out to investigate the electrochemical reduction of disperse nitro dyes in [C_4mpyrr][NTf_2], with the aim of investigating the effect of the RTIL cation on the stability of the radical anion and dianion.

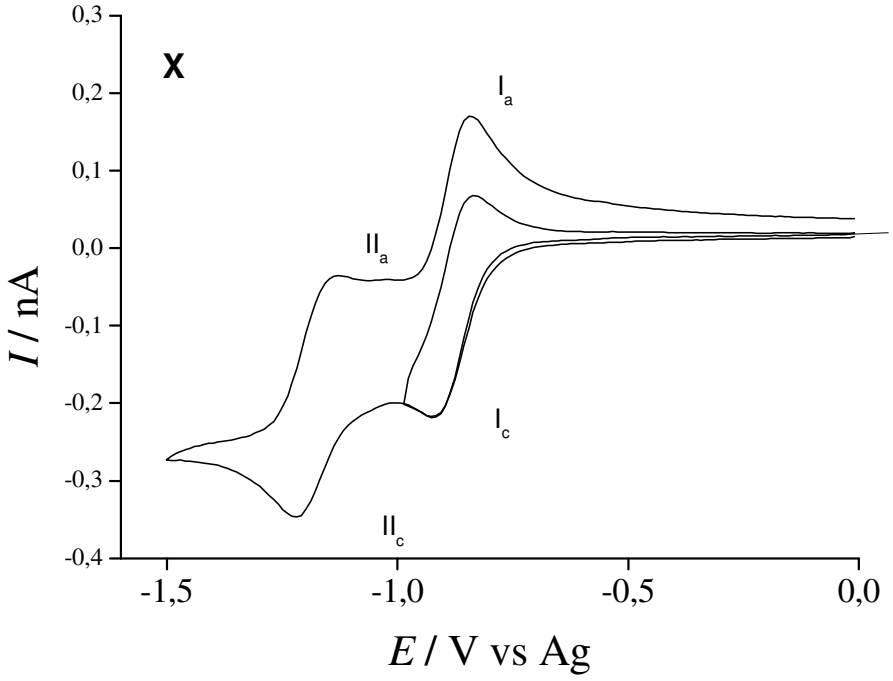

Figure 12. Cyclic voltammograms for the reduction of 10 mM Red13 in [C_4mpyr][NTf_2] on a Pt microelectrode at a scan rate of 100 mV s^{-1}.

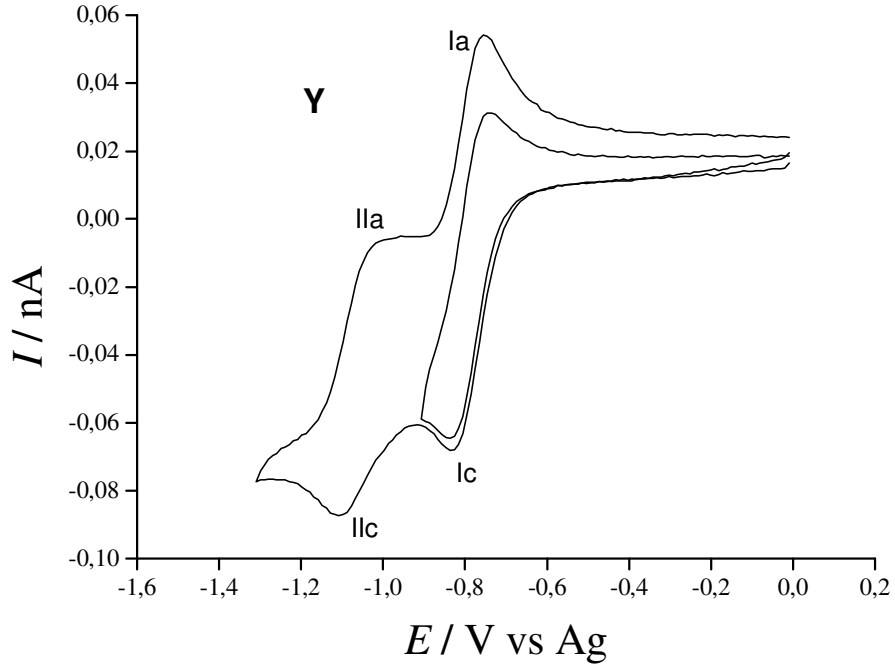

Figure 13. Cyclic voltammograms for the reduction of 10 mM Red1 in $[C_4mpyr][NTf_2]$ on a Pt microelectrode at a scan rate of 100 mV s^{-1}.

The voltammograms obtained for reduction of 10 mM Red1, Red13 and Or1 dyes in $[C_4mpyrr][NTf_2]$ on Pt microelectrode are shown in Figures 12, 13 and 14 respectively. The curves obtained for Red13 (Figure 12) and Red1 (Figure 13) and are fairly similar to those obtained in $[C_4mim][NTf_2]$ and present two reversible reduction peaks at potentials of -0.62 V *vs* Fc/Fc^+ (I_c) and -0.92 V *vs* Fc/Fc^+ (II_c) for Red13 and -0.68 V *vs* Fc/Fc^+ (I_c) and -0.98 V *vs* Fc/Fc^+ (II_c) for Red1. The ratio of I_a/I_c and II_a/II_c is close to unity and the peak current increases linearly with square root of scan rate from 10 to 2000 mV s^{-1}. Both waves indicate that Red1 and Red13 are being reduced in a similar way to that proposed in Equations 1 and 2, generating the respective radical anion and dianion. However, Or1 is reduced in three cathodic steps in $[C_4mpyrr][NTf_2]$, as shown Figure 14 . The corresponding $E_{1/2}$ values of -0.64 V *vs* Fc/Fc^+ (I_c) and -0.91 V *vs* Fc/Fc^+ (II_c) for Orange1 was obtained. The first peak (I_c) presents an anodic peak (I_a) at a potential 60 mV less negative on the reverse scan, and the I_a/I_c are close to one at all scan rates, indicating the occurrence of a stable radical anion. The second reduction peak (II_c) presents an anodic peak (II_a) on the reverse scan that is significant only at scan rates higher than 1000 mV s^{-1}. In addition, a shoulder is seen at less negative potential that increases at slower scan rates, clearly indicating the occurrence of a disproportionation reaction of the dianion formed. A third cathodic peak is observed, labeled III_c, at a more negative potential of -1.22 *vs* Fc/Fc^+ which becomes more reversible at higher scan rate. The magnitude of the peak II_c decreases markedly while the reversibility of the second reduction step (II_c) increases at high

scan rate, indicating that the product of the following chemical reaction to the dianion formation is electroactive at more negative potentials (III_c).

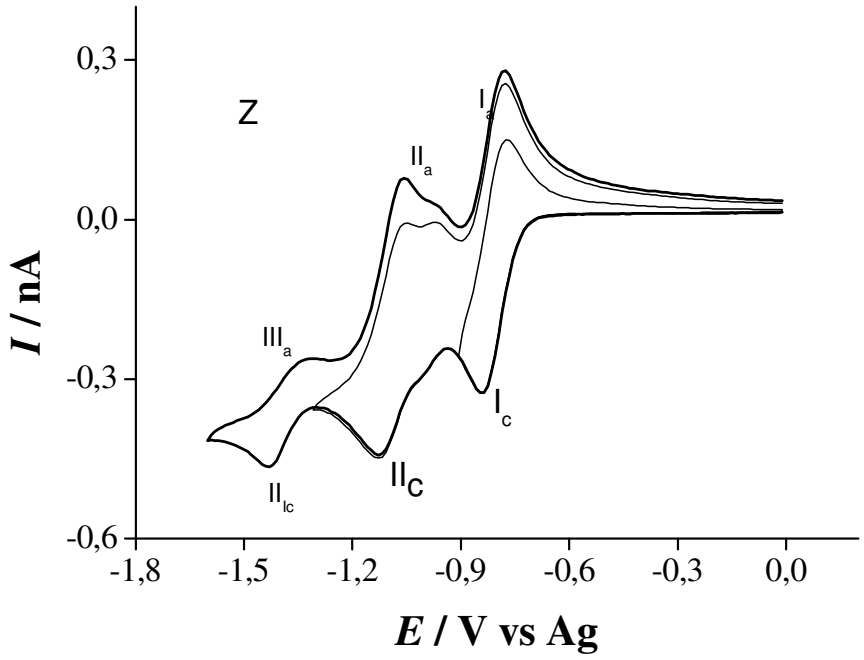

Figure 14. Cyclic voltammograms for the reduction of 10 mM Orange1 in $[C_4mpyr][NTf_2]$ on a Pt microelectrode at a scan rate of 100 mV s^{-1}.

Taking into consideration that the chemical structure of Or1 and Red1 differ only by an amine group, this behavior could be indicative that the dianion Or1 is susceptible to cleavage of the N-H bond of the secondary amine. Similar behavior was observed previously for N-n-butyl-4-nitrobenzenesulfonamide in aprotic medium [53]. The pyrrolidinium, $[C_4mpyrr]^+$, system is less acidic than the imidazolium, $[C_4mim]^+$, moiety since the two nitrogen atoms decrease the reactivity of the H located in position 2. Thus, the $[C_4mpyr][NTf_2]$ is a base strong enough to associate or remove protons from the mono-substituted amine group as in the case of Or1. Thus the third reductive process could be explained using equations (3) and (4) respectively.

$$[O_2NC_6H_4N{=}NC_6H_4NR]^{2-} + [C_4mpyrr]^+ \rightarrow [O_2NC_6H_4N{=}NC_6H_4NR]^- + [C_4mpyrr]H^+ \quad (3)$$

$$[O_2NC_6H_4N{=}NC_6H_4NR]^- + e^- \rightarrow [O_2NC_6H_4N{=}NC_6H_4NR]^{2-\bullet} \quad (4)$$

An overview of the electrochemical reduction of Or1 seems to show evidence that they undergo N-H cleavage only when the dianion is generated. The occurrence of bond cleavage observed for Or1 and slow dissociation of the dianion formed only in $[C_4mpyr][NTf_2]$ indicates that the

electrochemical reduction of nitro aromatics compounds cannot be generalized, but the anion radicals are stable enough to allow the transfer of a second electron.

4. CONCLUSIONS

An overview of the electrochemical reductions of disperse azo dyes Red1, Red13 and Orange1 in the ionic liquids $[C_4mim][N(Tf)_2]$ and $[C_4mpyrr][N(Tf)_2]$ seems to show evidence that they undergo a one electron reversible step to form a radical anion stable enough for allowing the transfer of a second electron in a separate step, in contrast with other aprotic medium as DMF, that present almost complete suppression of the dianion radical. Despite forming the dianion radical with relatively high stability in RTILs, there was evidence that a cleavage reaction involving the N-H substituent on secondary amine of Orange1 in $[C_4mpyrr][N(Tf)_2]$ alters the route observed for all other dyes. The large difference in the stabilities between secondary amine radical anions implies that the ease with which nitrogen-hydrogen bond cleavage occurs is easily rationalised on the basis of their acidities. Their influence on nitro reduction is explained due to high electron delocalisation in the molecule. The potentials required for reduction and oxidation represent the different electron withdrawing power of the substituents in the dyes analyzed, but while the reductive facility of the nitro group seems to be inversely proportional to the mutagenic responses of the three disperse dyes for the strain TA 98 in the assays without exogenous metabolization, the oxidation of amine substituent on the dye seems to be directly dependent of the detected mutagenic activity.

ACKNOWLEDGMENTS
We thank the FAPESP and CNPq, Brazil, for the financial support.

References

1. H. Zollinger, Color Chemistry - Synthesis, Properties and Applications of Organic Dyes and Pigments, V. C. H., New York, 1991.
2. R. O. A Lima, A.P. Bazo, D.M.F. Salvadori, C.M. Rech, D.P. Oliveira, DG.A. Umbuzeiro, G. A., *Mutat. Res*. 626 (2007) 53.
3. A. Matsuoka, A. Tada, Y. Terao, H. Nukaya, A. Onfelt, K. Wakabayashi, *Mutat. Res.* 493 (2001) 75.
4. T. Morisawa, T. Mizuno, T. Ohe, T. Watanabe, T. Hirayama, H. Nukaya, T. Shiozawa, Y. Terao, H. Sawanashi, K. Wakabayashi, K., *Mutat. Res.* 534 (2003)123.
5. H. Nukaya, T. Shiozawa, A. Tada, Y. Terao, T. Ohe, T. Watanabe, M. Asanoma, H. Sawanishi, T. Katsuhara, T. Sugimura, K. Wakabayashi, K., *Mutat. Res.* 492 (2001) 73.
6. D. P.Oliveira, P.A. Carneiro, C.M. Rech, M.V.B.; Zanoni, L.D.Claxton, G.A. Umbuzeiro, *Environ. Sci. Tech.* 40 (2006) 6682.
7. D.P. Oliveira, P.A. Carneiro, M. Sakagami, M.V.B. Zanoni, G.A. Umbuzeiro, *Mutat. Res.* 626 (2007) 135.
8. D.P. Oliveira, M. Kuhlmann, G.A. Umbuzeiro, *Soil Sediment Contam.* 15 (2006) 455.
9. T. Shiozawa, K. Suyama, K. Nakano, H. Nukaya, H. Sawanishi, A. Oguri, K. Wakabayashi, Water. Mutat. Res. 442 (1999)105.

10. T. Shiozawa, A. Tada, H. Nukaya, T. Watanabe, Y.Takahashi, M. Asanoma, T. Ohe, H. Sawanashi, T. Katsuhara, T. Sugimura, K. Wakabayashi, Y. Terao, Y. Chem. *Res. Toxicol.* 13 (2000) 535.
11. M.S. Tsuboy, P.F. Angeli, M.S.; Mantovani, S. Knasmuller, G.A. Umbuzeiro, L.R. Ribeiro, L. R., *Toxicology in vitro* 21 (2007) 1650.
12. G.A. Umbuzeiro, C.A. Coimbrão, F. Kummrow, D.J.A. Lobo, P.H.N. Salvida, *J. Braz. Soc. Ecotox.* 2 (2007) 163.
13. G.A. Umbuzeiro, H. Freeman, S. Warren, L.D. Claxton, *Food Chem. Toxicol.* 43 (2005) 49.
14. G.A. Umbuzeiro, H. Freeman, S.Warren, D.P. Oliveira, Y. Terao, T. Watanabe, L.D. Claxton, *Chemosphere* 60 (2005) 55.
15. G.A. Umbuzeiro, F. Kummrow, D.A. Roubicek, M.Y. Tominaga, Environ. Internat. 32 (2006) 359.
16. G.A. Umbuzeiro, D.A. Roubicek, C.M. Rech, M.I.Z. Sato, L.D. Claxton, *Chemosphere* 54 (2004) 1589.
17. G.A. Umbuzeiro, S. Warren, L.D. Claxton, *Mutat. Res. Genetic Toxicol. Environ. Mutagenesis* 609 (2006) 26.
18. T. Watanabe, H. Nukaya, Y. Terao, Y. Takahashi, A. Tada, T. Takamura, H. Sawanashi, T. Ohe, T. Hirayama, T. Sugimura, K. Wakabayashi, *Mutat. Res.* 498 (2001) 107.
19. T. Watanabe, T. Shiozawa, Y. Takahashi, T. Takahashi, Y. Terao, H. Nukaya, T. Takamura, H. Sawanashi, T. Ohe, T. Hirayama, K. Wakabayashi, *Mutagenesis* 17 (2002) 293.
20. T. Watanabe, Y. Takahashi, T.; Takahashi, H. Nukaya, Y. Terao, T. Hirayama, K. Wakabayashi, *Mutat. Res.* 519 (2002) 187.
21. K. Hunger,. *Chimia* 48 (1994) 520.
22. F. Rafii, J.D. Hall, C.E.; Cerniglia, *Food Chem. Toxicol.* 35 (1997) 897.
23. S. Zbaida, *Drug Metab. Rev.* 27 (1995) 497.
24. S. Zbaida, W.G. Levine, *Chem. Res. Toxicol.* 4 (1991) 82.
25. M.C. Buzzeo, R.G. Evans, R. G. Compton,. *Chem Phys Chem* 5 (2004) 1106.
26. P. Hapiot, C. Lagrost, *Chem. Rev.* 108 (2008) 2238.
27. D.S. Silvester, R.G. Compton, *Z. Phys. Chem.* 220 (2006) 1247.
28. D.S. Silvester, E.I. Rogers, L.E. Barrosse-Antle, T.L. Broder, R.G. Compton, *J. Braz. Chem. Soc.* 9 (2008) 611.
29. A.M. O'Mahony, D.S. Silvester, L. Aldous, C. Hardacre, R.G. Compton, *J. Chem. Eng. Data* 53 (2008) 2884.
30. E.I. Rogers, B. Šljukić, C. Hardacre, R.G. Compton, *J. Chem. Eng. Data* 54 (2009) 2049.
31. C.A. Brooks, A.P. Doherty, *J. Phys. Chem.* B 109 (2005) 6276.
32. C. Lagrost, D. Carrié, M. Vaultier, P. Hapiot, *J. Phys. Chem.* A 107 (2003) 745.
33. C. Lagrost, P. Hapiot, M.Vaultier, *Green Chem.* 7 (2005) 468.
34. D. Zigah, J. Ghilane, C. Lagrost, P Hapiot, *J. Phys. Chem.* B 112 (2008) 14952.
35. M.C. Buzzeo, O.V. Klymenko, J.D. Wadhawan, C. Hardacre, K.R. Seddon, R.G. Compton, *J. Phys. Chem. A* 1037 (2003) 8872.
36. P. Bonhôte, A.P. Dias, N. Papageorgiou, K. Kalyanasundaram, M. Grätzel, *Inorg. Chem.* 35 (1996) 1168.
37. M. Sharp, *Electrochim. Acta* 28 (1983) 301.
38. U.Schröder, J.D. Wadhawan, R.G. Compton, F. Marken, P.A.Z. Suarez, C.S. Consorti, J. Dupont, *New J. Chem.* 24 (2000) 1009.
39. D. Shoup, A. Szabo, *J. Electroanal. Chem.* 140 (1982) 237.
40. R.G.Evans, O.V. Klymenko, S.A. Saddoughi, C. Hardacre, R.G. Compton, *J. Phys. Chem.* B 108 (2004) 7878.
41. R.G. Evans, O.V. Klymenko, C. Hardacre, K.R. Seddon, R.G. Compton, *J. Electroanal. Chem.* 556 (2003) 179.

42. R.G. Evans, O.V. Klymenko, P.D. Price, S.G. Davies, C. Hardacre, R.G. Compton, *Chem. Phys. Chem.* 6 (2005)526.
43. M.M. Baizer, H. Lund, Organic Electrochemistry: an Introduction and a Guide. 2nd ed.; Marcel Dekker: New York, 1983.
44. C.L. Forryan, N.S. Lawrence, N. V. Rees, R.G. Compton, *J. Electroanal. Chem.* 561 (2004) 53.
45. D.S. Silvester, A.J. Wain, L. Aldous, C. Hardacre, R.G. Compton, *J. Electroanal. Chem.* 596 (2006) 131.
46. C. Lagrost, L. Preda, E. Volanschi, P. Hapiot, *J. Electroanal. Chem.* 587 (2005) 1.
47. P. Zuman, Z. Fijalek, *J. Electroanal. Chem*. 296 (1990) 583.
48. G. Gritzner, J. Kuta, *Pure Appl. Chem.* 56 (1984) 461.
49. M.E. Osugi, M.V.B. Zanoni, C.R. Chentamarakshan, N.R. Tacconi, G.A.; Woldemariam, S.S. Mandal, K. Rajeshwar, K., *J. Adv. Oxid. Tech.* 11 (2008) 425.
50. L.F.R. Pinto, I. Felzenszwalb, in: Mutagenese Ambiental, Ribeiro, L. R.; Salvadori, D. M. F.; Marques, E. K., Eds. Editora da Ulbra, 2003.
51. M. Rudolph, D.P. Reddy, S.W. Feldberg, *Anal. Chem.* 66 (1994) 589.
52. J.A. Alden, F. Hutchinson, R.G. Compton, *J. Phys. Chem*. B 101 (1997) 949.
53. M.V.B. Zanoni, N.R. Stradiotto, *J. Electroanal. Chem.* 312 (1991) 141.